Photoisomerization of Azobenzene Grafted to Layered Silicates: Simulation and Experimental Challenges

Hendrik Heinz,*[,†,‡] R. A. Vaia,[†] H. Koerner,[†,§] and B. L. Farmer[†]

Materials and Manufacturing Directorate, Air Force Research Laboratory, Wright Patterson AFB, Ohio 45433, and Department of Polymer Engineering, University of Akron, Akron, Ohio 44325

Received May 12, 2008. Revised Manuscript Received September 4, 2008

Molecular dynamics (MD) simulation has been employed to examine the molecular-level orientation and reorganization of model azobenzene derivatives in the interlayer space of layered silicates upon laser excitation in comparison with existing X-ray diffraction data and UV/vis absorption measurements. MD results show uniform reversible changes in basal plane spacing of montmorillonite up to 2.8 Å (14%) upon trans−cis isomerization of attached photoactive surfactants such as (4,4′-phenylazophenyl)-diammonium ions and (4-phenylazophenyl)ammonium ions. Uniform, significant reponses are supported by the presence of cointercalate to compensate changes in interlayer density, by conformational rigidity and upright orientation of the azobenzene-containing surfactants on the mineral surface, and a medium-to-high packing density. Experimentally, Okada et al. have shown nonuniform reversible optical switching of the gallery height for semiflexible surfactants up to 10 Å (41%) in the presence of phenol and uniform reversible optical switching of 0.9 Å (4%) without cointercalates [Okada et al. *J. Mater. Chem.* **2005**, *15*, 987−992]. Further experimental data also show the absence of changes in gallery spacing for azobenzene derivatives with attached flexible hydrocarbon chains at low packing density without cointercalates and are explained by simulation. From a methods viewpoint, an approach is introduced to simulate the photoisomerization reaction using classical molecular dynamics, taking quantitatively into account the input of photon energy, the time scale of the isomerization (∼1 ps), and the relative energies of the trans and of the cis isomer, as well as the thermal conversion barrier. A temporary modification of the C−N═N−C torsion potential describes the input of photon (excitation) energy, which can be applied to common force fields (including PCFF, OPLS-AA, COMPASS, CVFF, AMBER, CHARMM) and facilitates the simulation of the photoisomerization reaction as a function of molecular environment, pressure, temperature, and excitation time.

1. Introduction

Novel optic and photonic materials as well as new technologies for sensors and actuators rely on the responses of molecular-scale assemblies to external stimuli.[1−3] Responsive devices and molecular structures have been prepared in numerous ways,[4−12] for example, electrolysis cells with pressure responses to an applied voltage,[8] voltage-sensitive strips with deflection responses,[10] carbon nanotube−polymer composites with strain responses to IR radiation and electric fields,[12] photosensitive coatings with motion responses,[9] and molecular switches involving azobenzene.[5] The trans−cis isomerization of azobenzene upon irradiation with UV or visible light is a key event in switching of molecular nanostructures, memory-shape polymers, and in data storage applications.[4−7,9,13,14]

In this work, we have examined layered silicate structures with switchable gallery spacing upon laser irradiation, which contain intercalated azobenzene as a photoresponsive center (Figure 1).[13,14] Azobenzene undergoes reversible cis−trans isomerization upon optical pumping which is known to induce phase transitions in liquid crystals[4−6] and in various polymers.[5,7,9,11,13,14] The combination with layered silicates, which form even surfaces extended up to hundreds of nanometers,[15,16] can introduce spatially uniform responses

* Corresponding author. E-mail: hendrik.heinz@uakron.edu.
† Wright Patterson AFB.
‡ University of Akron.
§ Also at Universal Technology Corp., Dayton, OH 45432.

(1) Wilson, M.; Kannangara, K.; Smith, G.; Simmons, M.; Raguse, B. *Nanotechnology* Chapman and Hall: Boca Raton, 2002.
(2) *Actuators*; Janocha, H., Ed.; Springer: Berlin, 2004.
(3) (a) Dai, L. *Intelligent Macromolecules for Smart Devices*; Springer: London, 2004. (b) Koerner, H.; White, T. J.; Tabiryan, N. V.; Bunning, T. J.; Vaia, R. A. *Mater. Today* **2008**, *11*, 34–42.
(4) Ikeda, T.; Tsutsumi, O. *Science* **1995**, *268*, 1873–1875.
(5) Feringa, B. L.; van Delden, R. A.; Koumura, N.; Geertsema, E. M. *Chem. Rev.* **2000**, *100*, 1789–1816.
(6) Ichimura, K.; Oh, S.-K.; Nakagawa, M. *Science* **2000**, *288*, 1624–1626.
(7) Liang, X.; Asanuma, H.; Komiyama, M. *J. Am. Chem. Soc.* **2002**, *124*, 1877–1883.
(8) Cameron, C. G.; Freund, M. S. *Proc. Natl. Acad. Sci. U.S.A.* **2002**, *99*, 7827–7831.
(9) Hugel, T.; Holland, N. B.; Cattani, A.; Moroder, L.; Seitz, M.; Gaub, H. E. *Science* **2002**, *296*, 1103–1106.
(10) Fukushima, T.; Asaka, K.; Kosaka, A.; Aida, K. *Angew. Chem., Int. Ed.* **2005**, *44*, 2410–2413.
(11) Kraeutler, V.; Aemissegger, A.; Huenenberger, P. H. *J. Am. Chem. Soc.* **2005**, *127*, 4935–4942.
(12) Ahir, S. V.; Terentjev, E. M. *Nat. Mater.* **2005**, *4*, 491–495.
(13) Nuyken, O.; Scherer, C.; Baindl, A.; Brenner, A. R.; Dahn, U.; Gartner, R.; Kaiser-Rohrich, S.; Kollefrath, R.; Matusche, P.; Voit, B. *Prog. Polym. Sci.* **1997**, *22*, 93–183.
(14) Natansohn, A.; Rochon, P. *Chem. Rev.* **2002**, *102*, 4139–4175.
(15) Hydrous Phyllosilicates. In *Reviews in Mineralogy*; Bailey, S. W, Ed.; Mineralogical Society of America: Chelsea, MI, 1988; Vol. 19 (see also http://www.webmineral.com).

10.1021/cm801287d CCC: $40.75
Published on Web 10/04/2008

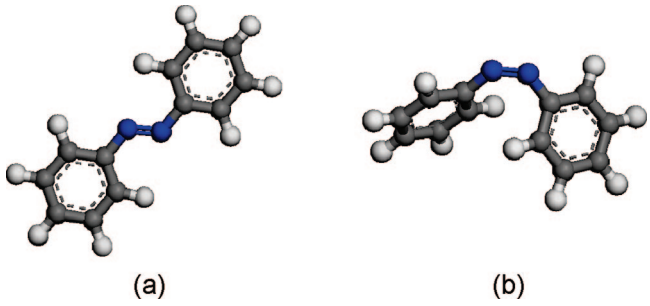

Figure 1. (a) Trans isomer and (b) cis isomer of azobenzene.

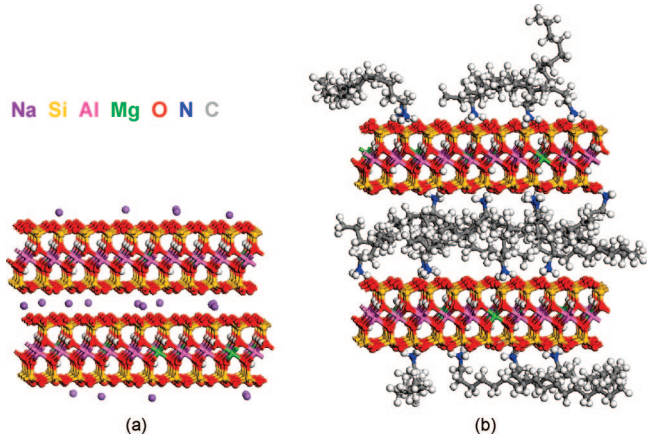

Figure 2. Molecular structure of (a) sodium montmorillonite (cation exchange capacity 91 mequiv/100 g) and (b) *n*-dodecylammonium montmorillonite, viewed along the *y* axis. The gallery spacing of the layered structure depends on the grafting density and on the molecular volume of the cationic surfactant.

in one dimension. Such hybrid structures can be prepared by exchange of alkali ions on the layered silicate surface with suitable ammonium surfactants containing azobenzene (Figure 2).[17−20]

The synthesis and characterization of hybrid structures of this kind have been carried out; however, it has been difficult to evaluate and control the location and the orientation of the intercalated azo dyes using X-ray and UV/vis spectroscopy.[17−20] While effective photoisomerization in the interlayer space has been confirmed by bleaching the corresponding absorptions in UV/vis spectroscopy, measurements of reversible changes in gallery height range between 0 and 10 Å (0−41%). The largest changes are induced by cointercalation of additives such as phenol, although the increase only occurs in parts of the sample and is not uniform.[20] Without cointercalates, the geometry of trans and cis azobenzene (Figure 1) suggests the possibility of a reversible change in length of ∼2.3 Å and higher for substituted azobenzene, while only up to 0.9 Å (4%) has been observed experimentally.[18] In addition, conversion times have been rather long

Scheme 1. Cationic Surfactants Chosen in the Simulation

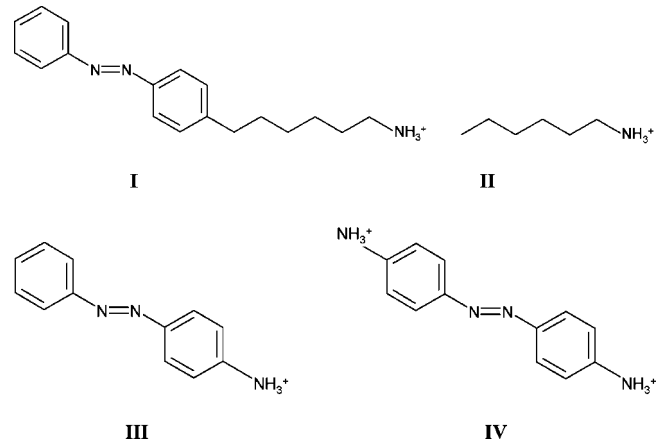

(30 min) compared to the isomerization in the gas phase which proceeds on the order of 1 ps or 100 ps, after several laser pulses for quantitative conversion, respectively. Therefore, the interpretation of available experimental data, the structure of the interlayer, and the isomerization dynamics by molecular simulation can provide guidance toward the design of more efficient photoresponsive structures, which may find application as nanoscale switches or actuators.

The interlayer space of phyllosilicates has been previously explored using molecular simulation methods, and the quantitative explanation of experimental data including X-ray diffraction (XRD), IR, sum frequency generation (SFG), differential scanning calorimetry (DSC), near-edge X-ray absorption fine structure (NEXAFS), surfactant tilt angles, and surface energies has been demonstrated.[21−31] We aim at the examination of the structural changes of representative azobenzene-containing cationic model surfactants (Scheme 1) in the interlayer space of phyllosilicates during the trans−cis conversion, using classical molecular dynamics simulation and a novel approximation of the reaction path. Computed orientations of intercalated azobenzene moieties compare favorably to experimental UV/vis solvatochromic shifts, and changes in basal plane spacing are in agreement with results of X-ray measurements. The results increase the understanding of the isomerization reaction within the gallery, provide estimates for possible reversible changes in basal plane spacing, and suggest conditions for uniform, reversible switching.

(16) Lagaly, G.; Jasmund, K. *Tone und Tonminerale*; Steinkopff: Darmstadt, 1993.
(17) Ogawa, M.; Ishii, T.; Miyamoto, N.; Kuroda, K. *Adv. Mater.* **2001**, *13*, 1107–1109.
(18) Iyi, N.; Fujita, T.; Yelamaggad, C. V.; Lopez Arbeloa, F. *Appl. Clay Sci.* **2001**, *19*, 47–58.
(19) Ogawa, M.; Ishii, T.; Miyamoto, N.; Kuroda, K. *Appl. Clay Sci.* **2003**, *22*, 179–185.
(20) Okada, T.; Watanabe, Y.; Ogawa, M. *J. Mater. Chem.* **2005**, *15*, 987–992.
(21) Hackett, E.; Manias, E.; Giannelis, E. P. *J. Chem. Phys.* **1998**, *108*, 7410–7415.
(22) Heinz, H.; Castelijns, H. J.; Suter, U. W. *J. Am. Chem. Soc.* **2003**, *125*, 9500–9510.
(23) Zeng, Q. H.; Yu, A. B.; Lu, G. Q.; Standish, R. K. *Chem. Mater.* **2003**, *15*, 4732–4738.
(24) Heinz, H.; Suter, U. W. *J. Phys. Chem. B* **2004**, *108*, 18341–18352.
(25) Heinz, H.; Suter, U. W. *Angew. Chem., Int. Ed.* **2004**, *43*, 2239–2243.
(26) He, H.; Galy, J.; Gerard, J-F. *J. Phys. Chem. B* **2005**, *109*, 13301–13306.
(27) Pandey, R. B.; Anderson, K. L.; Heinz, H.; Farmer, B. L. *J. Polym. Sci., Part B* **2005**, *43*, 1041–1046.
(28) Heinz, H.; Koerner, H.; Vaia, R. A.; Anderson, K. L.; Farmer, B. L. *Chem. Mater.* **2005**, *17*, 5658–5669.
(29) Heinz, H.; Vaia, R. A.; Farmer, B. L *J. Chem. Phys.* **2006**, *124*, 224713: 1–9.
(30) Heinz, H.; Vaia, R. A.; Krishnamoorti, R.; Farmer, B. L. *Chem. Mater.* **2007**, *19*, 59–68.
(31) Heinz, H.; Vaia, R. A.; Farmer, B. L. *Langmuir* **2008**, *24*, 3727–3733.

We consider conformationally flexible alkyl-modified azobenzene derivatives as well as conformationally rigid azobenzene derivatives as model surfactants in the layered silicate galleries (Scheme 1). They are similar to conformationally flexible and semiflexible experimental systems (see section 5)[17−20] and include structural features to potentially improve switching. The flexible model surfactants include mixtures of 6-(4-phenylazophenyl)hexylammonium ions (**I**) and *n*-hexylammonium ions (**II**) on a montmorillonite surface with a low cation exchange capacity (CEC = 91 mequiv/100 g, Southern Clay).[30] The rigid surfactants include (4-phenylazophenyl)ammonium ions (**III**) and (4,4′-phenylazophenyl)diammonium ions (**IV**) on a montmorillonite surface with a higher CEC (143 mequiv/100 g, Nanocor).

The outline of the paper is as follows. In section 2, we examine the trans−cis isomerization and describe a quantitative approach to simulate the reaction path using classical force fields. Section 3 contains details of the computational models and procedures. In section 4, we discuss results of molecular dynamics simulation of montmorillonite modified with azobenzene derivatives. Section 5 follows with a comparison of the results to experimental data and suggestions to increase reversible actuation. The paper concludes with a summary in section 6.

2. Simulation of the Trans−Cis Conversion of Azobenzene

The difference in geometry between the two isomers (Figure 1) is well reproduced by DFT calculations[32] and by semiempirical classical simulation, for example, using the polymer consistent force field (PCFF).[33] The trans isomer is planar while the cis isomer departs from planar shape; the benzene rings are twisted relative to each other to avoid close contacts between the ring hydrogen atoms. The changes in longitudinal extension of 2.3 Å as well as in twist upon isomerization determine the potential of reversible switching in self-assembled structures.

A physically meaningful simulation of the trans−cis isomerization will comprise the input of photon energy into the system and the rotation of the C−N=N−C azo bond in response to the excitation, consistent with the functional form of the energy expression (Hamiltonian). We present a near-quantitative description of this process using classical molecular dynamics simulation and available terms in common force fields (PCFF, OPLS-AA, COMPASS, CVFF, AMBER, CHARMM) which can be applied to large systems (currently up to $\sim 10^6$ atoms). We begin with a brief review of the photoisomerization reaction, outline the computational model, discuss simple test systems, and summarize the utility and limitations of the proposed model.

2.1. Course of the Photoinduced Reaction. The trans−cis isomerization of azobenzene and electronically homologous stilbene have been studied by femtosecond laser spectroscopy, NMR, and ab initio calculations.[5,9,34−36] A schematic overview by Hugel et al. is shown in Figure 3.[9]

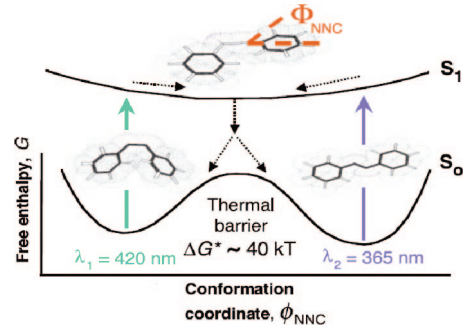

Figure 3. Laser-induced conversion of azobenzene according to Hugel et al. (ref 9). Instead of the N=N−C angle, we consider the C−N=N−C dihedral angle as a reaction coordinate (refs 34 and 35).

Upon excitation with a femtosecond laser pulse, the molecule is brought into the first excited state. The energy minimum of the excited state occurs at a C−N=N−C dihedral angle $\varphi = 90°$, from which the molecule decays to the ground state, and the product branches either to the trans ($\varphi = 180°$) or to the cis form ($\varphi = 0°$) with equal probability.[34,35] The time scale for the overall reaction ranges between several 100 fs to 2 ps, depending on the substitution pattern.[34,35] As shown in Figure 3,[9] the trans isomer of lowest energy requires electromagnetic radiation of higher energy (365 nm) to reach the excited state compared to the cis isomer which is of higher energy and requires radiation of lower energy (420 nm). Therefore, effectively full conversion in either direction can be achieved by applying femtosecond pulses of the appropriate wavelength repeatedly in intervals on the order of ps.

2.2. Implementation in Molecular Dynamics Simulation. The time scale of 1 ps for the isomerization is compatible with semiempirical classical molecular dynamics simulation which typically employs a time step of 1 fs and total simulation times on the order of 1 ns or more.

The reaction coordinate can be described by the C−N=N−C torsion angle φ, which changes from $\varphi = 180°$ (trans) to $\varphi = 0°$ (cis) during a trans → cis conversion and vice versa for a cis → trans conversion. A temporary modification of the torsion potential in the semiempirical energy expression provides a simple model for the reaction path. In contrast to the repetition of many laser pulses in experiment and branching to the trans or to the cis conformation with equal probability at each occurrence, we focus on one constant stimulus over a given period of time in only one direction, either in the trans → cis direction or in the cis → trans direction.

A commonly used functional form of the torsion potential is the three-term torsion potential, for example, in the polymer consistent force field (PCFF) and similarly in the OPLS-AA and COMPASS force fields:

$$E_\varphi = k_{\varphi 1}[1 - \cos(1\varphi - \varphi_{01})] + k_{\varphi 2}[1 - \cos(2\varphi - \varphi_{02})] + k_{\varphi 3}[1 - \cos(3\varphi - \varphi_{03})] \quad (1)$$

This expression is advantageous over a one-term torsion potential because the intrinsic energy difference of 10.3 kcal/

(32) *Dmol3* as implemented in *Materials Studio*, Version 3.2; Accelrys, Inc.: San Diego, CA, 2003.
(33) *Cerius2* and *Discover* program. *Discover User Guide*, Version 96.0/4.0.0; Accelrys, Inc.: San Diego, CA, 2003.
(34) Waldeck, D. H. *Chem. Rev.* **1991**, *91*, 415–436.
(35) Dou, Y.; Allen, R. E. *J. Chem. Phys.* **2003**, *119*, 10658–10666.

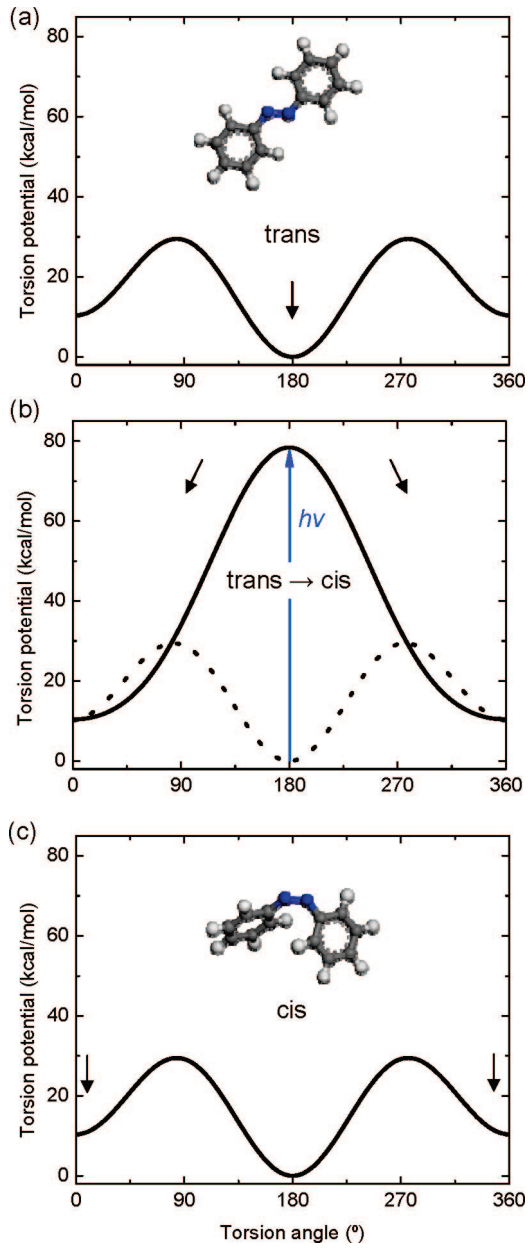

Figure 4. Modification of the C—N═N—C torsion potential to simulate the trans → cis isomerization using a classical force field. (a) The trans isomer, (b) the response to an excitation, and (c) the cis isomer. A barrier of height $E = h\nu$ at $\varphi = 180°$ is raised to convert trans-configured double bonds into cis-configured double bonds, representing the input of photon energy $h\nu$.

mol between the cis and the trans isomer as well as the thermal conversion barrier of ~24 kcal/mol can be taken into account.[9] Similar to the relative stability of the diastereomers, the photon energy $E = h\nu$ corresponding to the HOMO−LUMO difference can be used as an input for a torsion barrier to initiate a trans → cis or a cis → trans isomerization (Figure 4). The sets of parameters for the thermal equilibrium state, the trans → cis isomerization, and the cis → trans isomerization are shown in Table 1. Molecular dynamics simulation of trans-azobenzene and cis-azobenzene in the gas phase at 298 K indicates that nonbond interactions (van der Waals and Coulomb) exert no influence on the relative energies of the isomers within ±0.2 kcal/mol so that stepwise changes in the torsion potential alone are sufficient to describe the reaction.

We discuss the simulation of the excitation process for a trans → cis conversion as an example in detail (Figure 4). At the outset, the structure containing trans-azobenzene ($\varphi = 180°$) is subjected to molecular dynamics simulation so that an equilibrium trajectory is obtained (Figure 4a) using the C—N═N—C dihedral parameters $k_{\varphi 1} = 5.2$ kcal/mol, $\varphi_{01} = 180°$, $k_{\varphi 2} = 12$ kcal/mol, $\varphi_{02} = 0°$, $k_{\varphi 3} = 0$ kcal/mol, and $\varphi_{03} = 0°$ (Table 1). Then, the torsion potential (eq 1) is modified to introduce a potential barrier at $\varphi = 180°$. This barrier approximates the excited-state energy of $E_{LUMO} - E_{HOMO} = h\nu = 328$ kJ/mol (78 kcal/mol) corresponding to a 365 nm photoexcitation (Figure 4b). The first term in eq 1 (order $n = 1$) represents this excitation energy in combination with the second term (order $n = 2$) which also maintains the energy level of cis-azobenzene. We assume that all molecules are excited at the same time and change the torsion potential to $k_{\varphi 1} = 34$ kcal/mol, $\varphi_{01} = 0°$, $k_{\varphi 2} = 5.2$ kcal/mol, $\varphi_{02} = 180°$, $k_{\varphi 3} = 0$ kcal/mol, and $\varphi_{03} = 0°$ (Table 1). Molecular dynamics simulation under the excited-state conditions is continued for 10 ps or other duration depending on the purpose of study, in which some or all molecules arrive at the cis configuration $\varphi = 0°$ (360°). The barrier of the torsion potential at $\varphi = 180°$ is subsequently lowered to arrive at the ground-state torsion potential, and the system is subjected to molecular dynamics simulation for equilibration using the parameters for thermal equilibrium for the C—N═N—C torsion (Figure 4c, Table 1).

Analogous to the trans → cis conversion, the cis → trans conversion can be simulated by increasing the torsion potential at $\varphi = 0°$ by 285 kJ/mol (68 kcal/mol) corresponding to a laser excitation at 420 nm wavelength. The original torsion parameters are temporarily changed to $k_{\varphi 1} = 34$ kcal/mol, $\varphi_{01} = 180°$, $k_{\varphi 2} = 0$ kcal/mol, $\varphi_{02} = 0°$, $k_{\varphi 3} = 0$ kcal/mol, and $\varphi_{03} = 0°$ (Table 1). Molecular dynamics is continued under the excited-state conditions for a given time (e.g., 10 ps), and then the potential is restored to the ground state.

As an alternative to the three-term torsion potential (eq 1), a simple one-term torsion potential, as found in the CVFF, CHARMM, and AMBER force fields, can also be applied:

$$E_\varphi = k_\varphi[1 + \cos(n\varphi - \varphi_0)] \qquad (2)$$

This one-term potential for the (Ph)C—N═N—C(Ph) torsion is also independent from nonbond interactions. However, the energy difference between the cis and the trans isomer must be neglected because of the simplicity of the functional form. The corresponding parameters for the simulation of the photoisomerization reaction are listed in Table 2.

2.3. Validation Using Simple Test Systems. For a first validation of molecular dynamics simulation of the photoisomerization reaction according to the outlined protocol, we consider models of crystalline, liquid, and gaseous azobenzene to examine the influence of excitation time, pressure, temperature, and molecular environment (Table 3).

The simulation of the isomerization reaction reveals distinct time scales for the trans−cis conversion and subsequent structural relaxation. Beginning with the initiation of

(36) Magennis, S. W.; Mackay, F. S.; Jones, A. C.; Tait, K. M.; Sadler, P. J. *Chem. Mater.* **2005**, *17*, 2059–2062.

Table 1. Parameters for the Three-Term Torsion Potential for the C−N=N−C Torsion (eq 1) To Simulate the Photochemical Conversion of Azobenzene

state	$k_{\varphi 1}$ (kcal/mol)	φ_{01} (deg)	$k_{\varphi 2}$ (kcal/mol)	φ_{02} (deg)	$k_{\varphi 3}$ (kcal/mol)	φ_{03} (deg)
thermal equilibrium	5.2	180	12	0	0	0
trans → cis (λ = 365 nm)	34	0	5.2	180	0	0
cis → trans (λ = 420 nm)	34	180	0	0	0	0

Table 2. Parameters for the One-Term Torsion Potential for the C−N=N−C Torsion (eq 2) To Simulate the Photochemical Conversion of Azobenzene[a]

state	k_φ (kcal/mol)	n	φ_0 (deg)
thermal equilibrium	12	2	180
trans → cis (λ = 365 nm)	39	1	180
cis → trans (λ = 420 nm)	39	1	0

[a] The energy difference between the trans and the cis isomer must be neglected in this potential due to the simplicity of the functional form.

the excitation, we can distinguish a "reaction time" in which the initially high energy drops and the transition from a C−N=N−C torsion angle $|\varphi| > 90°$ to a torsion angle $|\varphi| < 90°$ occurs, as well as a subsequent structural "relaxation time" in which the total energy relaxes to a new steady-state as an average over the azobenzene molecules in the simulation. Upon excitation, the half-life of the trans isomer is found to be between 60 and 90 fs. During this time, the bond rotation from trans to cis occurs, which sometimes appears like a twist of the azobenzene molecule because the C−N=N−C double bonds attempt quickly to assume the new configuration while the phenyl rings still remain in a position close to the old configuration. The formal reaction from trans to cis azobenzene is mostly complete after 200 to 300 fs, although the energy of the system has not reached equilibrium and subsequent relaxation of the structure takes between 1 and 10 ps. This period serves to remove initial strain and to position the phenyl rings in a low-energy cis configuration. If the excitation discontinues before the structural relaxation has made progress, the reaction may partially lead back to the original (trans) configuration.

Specific differences are seen depending on the state of aggregation (Table 3). In the gas phase, the reaction is faster and oscillations of the total energy occur during the relaxation period, both with and without usage of a thermostat for heat exchange. In the liquid state, the reaction is slightly slower than in the gas phase and a longer relaxation period is found with an initial drop in energy followed by a recovery period. In the solid state, reaction and relaxation times tend to be even longer. Under high pressure, the energy slowly decreases during a 10 ps relaxation period.

Heat exchange with the environment is also a critical factor in the photoisomerization reaction since the conversion of light into local heat raises the temperature to high values unless the system is coupled to a thermostat in the simulation for cooling. Relaxation times hence also depend on cooling rates, and the values in Table 3 are only a guide for primary relaxation processes under constant temperature. For example, transitions into new crystal structures or the relaxation of azobenzene-containing polymers upon photoisomerization may require much longer time to complete.

The computed conversion and relaxation times (Table 3) are in very good agreement with ab initio findings (section 2.1) and suggest interesting additional trends. Therefore, the model for the reaction path appears to be suitable to provide quantitative insight into the photoisomerization behavior of larger systems. We note, however, that only one-way conversions are taken into account and substantial energy barriers are involved (Figure 4b). A discussion of the reaction dynamics in greater depth as well as the exploration of variations of the model remains of interest for future research. For example, a reduction of the energy barriers in Tables 1 and 2 would lead to prolonged reaction times and less complete conversion. More details related to azobenzene-modified montmorillonite are discussed in section 4.

Computational Details for This Section. Model structures of trans-azobenzene were prepared as follows. For the crystal, X-ray data were employed[37] to build a 2 × 4 × 2 supercell of 2.43 × 2.30 × 3.08 nm^3 dimension. The solid was subjected to NPT dynamics at 298 K for thermal equilibration under two different pressures of 0 and 1 GPa (Table 3). (At 0 GPa, ∼5% deviations in computed cell parameters relative to experiment were noticed, indicating limitations of the PCFF model for azobenzene). The final structures were subjected to further NVT simulation under the given pressure, followed by the trans−cis conversion (100 ps) with the modified PCFF force field. For the liquid, 30 molecules of azobenzene were placed in a cubic box of ∼2 × 2 × 2 nm^3 dimension and equilibrated during 1 ns NPT molecular dynamics simulation at 373 K under two different pressures of 0 and 0.173 GPa. The final structures were subjected to further NVT simulation under the given pressure, and then the trans−cis conversion was induced under NVT conditions (100 ps). For the gas, 20 azobenzene molecules were randomly distributed in a box of $(10\ nm)^3$ size at 373 K and in a box of $(11.54\ nm)^3$ size at 573 K. The pressure in both cases was 101 kPa, the box size was determined using the ideal gas law, and the densities were 6.0 kg/m^3 and 3.9 kg/m^3. After equilibration in the NVT ensemble, the trans−cis isomerization was carried out (100 ps). In all simulations, the C−N=N−C torsion angles and the total energy were monitored as a function of excitation time.[38] The PCFF force field with C−N=N−C torsion potentials according to Table 2 was employed, using a time step of 1 fs, temperature control by velocity scaling (temperature window 10 K as well as ∞ for testing), and the Verlet integrator as implemented in the Discover program.[33] For molecular dynamics simulation in the NPT ensemble, the Parrinello-Raman barostat was employed.

2.4. Summary and Limitations. In summary, the rotation about the N=N bond is a suitable approximation to simulate trans → cis and cis → trans conversions of azobenzene and

(37) Brown, C. J. *Acta Crystallogr.* **1966**, *21*, 146–152.

(38) We have also tested a gradual increase of the torsion barrier to reach the full strength of the excitation and a gradual decrease after the specified time at full excitation. Smoothing the changes in energy in this manner does not affect the outcome of the simulation.

Table 3. Reaction and Relaxation Times of Azobenzene Model Systems upon Laser-Induced Trans−Cis Isomerization, Beginning at $t = 0$ fs, in Molecular Dynamics Simulation

state		reaction time[a] (fs)	average reaction time (fs) and half-life $t_{1/2}$[b] (fs)	relaxation time of the total energy (fs)[c]
gas (101 kPa)	373 K	35−200	80 [65]	160−800 (periodic fluctuation)
	573 K	35−160	70 [60]	200−1000 (periodic fluctuation)
liquid (373 K)	0.0 GPa	40−185	85 [75]	250−5000 (recovery)
	0.2 GPa	35−165	80 [70]	300−3000 (recovery)
solid (298 K)	0.0 GPa	35−185	85 [80]	300−1000 (weak fluctuation)
	1.0 GPa	45−320	95 [90]	600−10000 (slow decrease)

[a] Excitation time to transition from a C−N=N−C torsion angle $|\varphi| > 90°$ to a torsion angle $|\varphi| < 90°$. [b] Half-life in square brackets. [c] After a sharp initial drop in energy equal or close to the equilibrium value. Heat exchange with the environment was allowed to maintain a constant temperature.

azobenzene derivatives, mimicking the impact of multiple laser beams in experiment. Simulations with modified force fields are involved, which represent the temporary input of photon energy. The model is suitable to estimate conversion rates as a function of excitation time, external pressure, temperature, and molecular environment. The torsion parameters for the chemical reaction in Tables 1 or 2, respectively, can be adjusted to fit specific excited-state energies E (excitation wavelengths) for substituted azobenzenes according to $E = h\nu$. The total duration of the (single) excitation is an essential parameter in both simulation and experiment to determine the yield of the reaction (Table 3).[5,9,34−36,38]

In the described simulation protocol, all molecules are excited at the same time and a constant bias in one direction is applied (either trans → cis or cis → trans). In a real system, only some molecules are excited and then convert to reactant or product with equal likelihood. This random, two-way nature of the reaction could also be included in the simulation using stochastic excitation processes with dual outcomes (trans and cis), for example, through dynamic assignment of force field types for the C−N=N−C torsion (a set of reactive and a set of nonreactive atom types) and controlled rescaling of the reactive set of torsion parameters with extrema at $\varphi = 0°$, $|\varphi| = 90°$, and $|\varphi| = 180°$. Nevertheless, optical pumping in experiment typically comprises large numbers of repeated laser stimuli each of which induces significant reaction and relaxation times (section 2.1 and Table 3), and finally most molecules are converted. Therefore, a single temporary excitation in the simulation appears to be a reasonable first approximation.

The isomerization reaction leads to the addition and distribution of large amounts of energy locally so that thermostats are useful to extract heat from the system. A global thermostat such as velocity rescaling preserves local temperature gradients. If no heat exchange with the environment is desired, for example, to quantify the rate of energy transfer into regions close to the reaction centers, a large (∞) temperature window can be employed. Local thermostats may also be useful, and thermostats which periodically override local temperature gradients, such as the Andersen thermostat, are recommended with caution.

3. Computational Details

In the following, the preparation of the models, the simulation parameters, and the simulation protocols for the azobenzene-modified montmorillonites are described.

3.1. Models. Atomistic models of azobenzene and of the substituted ammonium ions **I** to **IV** were prepared using default parameters in the polymer consistent force field (PCFF) and new parameters for the C−N=N−C torsion (Table 1), using the Cerius^2 graphical interface.[33] Atomic charges on the primary ammonium head groups of $-0.5e$ (N), $+0.4e$ (H), and $+0.3e$ (C) were assigned according to dipole moments and the method of Heinz and Suter.[24,28]

Montmorillonite models were prepared according to the X-ray crystal structure.[39−42] The chemical composition equals $K_{0.333}[Si_4O_8][Al_{1.667}Mg_{0.333}O_2(OH)_2]$ for the cation exchange capacity (CEC) 91 mequiv/100 g (Southern Clay) and $K_{0.533}[Si_4O_8][Al_{1.467}Mg_{0.533}O_2(OH)_2]$ for the CEC 143 mequiv/100 g (Nanocor). The spatial distribution of Al → $Mg^- \cdots K^+$ charge defects in the octahedral sheet is implemented according to solid state NMR data.[25] Common uncertainties in CEC of ±5% and additional isomorphous substitution, for example, $Al^{3+} \rightarrow Fe^{3+}$,[39−42] in the corresponding natural minerals have a negligible effect on the outcome of this study. A detailed description of the models can be found in ref 28.

Models of the inorganic−organic hybrid structures were prepared in cubic boxes of $2.5959 \times 2.70459 \times 10$ nm^3 size, corresponding to a $5 \times 3 \times 1$ supercell of montmorillonite which is open in the z direction. Periodic boundary condition is effective in the x and y directions, and the open z direction permits free equilibration of the gallery spacing.[43]

The preparation of models for montmorillonite (CEC = 91 mequiv/100 g) modified with cations **I** and **II** was carried out in two steps. In the first step, a single montmorillonite layer with the trans-configured cations was prepared by replacing alkali metal ions with the surfactant cations on one side of the layer and with NH_4^+ ions for simplicity on the other side of the layer. The ammonium head groups of the surfactant ions were positioned at the same location as previous alkali metal ions. Several possibilities for the orientation of the surfactants **I** and **II** were tested; however, convergence of start structures with different chain orientation to the same average conformation and basal plane spacing was observed during molecular dynamics simulation due to short chain length. Following a brief energy mini-

(39) Rothbauer, R. *Neues Jahrb. Mineral., Monatsh.* **1971**, 143–154.
(40) Brown, G. *The X-ray Identification and Crystal Structures of Clay Minerals*; Mineralogical Society: London, 1961.
(41) Lee, J. H.; Guggenheim, S. *Am. Mineral.* **1981**, *66*, 350–357.
(42) Tipurski, S. I.; Drits, V. A. *Clay Miner.* **1984**, *19*, 177–193 (Mg positions not correct; see ref15 for an overview).
(43) Heinz, H.; Paul, W.; Suter, U. W.; Binder, K. *J. Chem. Phys.* **2004**, *120*, 3847–3854.

mization (200 steps steepest descent or conjugate gradient method), the single layer structures were subjected to NVT dynamics for 1 ns to relax the interface. In the second step, duplicate assemblies of two modified montmorillonite layers were prepared from two independent snapshots by uniformly offsetting coordinates and rotating one layer by 180° so that the surfactants on the inner side between the two layers were at a distance of several hundred picometers. The duplicate layers containing cations **I** and **II** were subjected to a short energy minimization (200 steps steepest descent or conjugate gradient method) and subsequent NVT molecular dynamics for 1 ns to reach equilibrium.

Models of montmorillonite (CEC = 143 mequiv/100 g) with surfactants **III** and **IV** were prepared for two distinct setups, one with perpendicular orientation of the rigid surfactants on the surface and vacuum to fill the remaining interlayer space and another with dense interlayer packing of the surfactants. The first set of models with upright orientation of the cations **III** and **IV** relative to the surface was prepared under consideration of three hydrogen bonds per ammonium group to the surface which stabilized the upright position. For montmorillonite-**III**, first a single layer and then duplicate layers were prepared similar to montmorillonite with cations **I** and **II**. For montmorillonite-**IV**, two parallel montmorillonite layers were directly placed at an interlayer distance so that the alkali metal ions on the inner surfaces could be replaced by cation **IV** in an upright orientation on the surface. The upright, duplicate structures were subjected to molecular dynamics for 1 ns and correspond to stable (local) energy minima. The vacuum to fill remaining interlayer space can thus be considered equal to a good implicit solvent. The second set of models with densely packed interlayers of cations **III** and **IV** was prepared similar to montmorillonite with cations **I** and **II**. For montmorillonite-**III**, the cations were oriented with a high tilt angle relative to the surface normal. For montmorillonite-**IV**, directly a duplicate assembly with dication **IV** in near-parallel orientation to the two surfaces was prepared and subjected to molecular dynamics for 1 ns. In this configuration, some dications form ionic bonds that cross-link the two silicate layers and others form two ionic bonds to the same silicate layer.

For montmorillonite-**III** and montmorillonite-**IV**, the relation between the two stable setups with upright orientation of the surfactants on the surface and with densely packed interlayer structure will be discussed in section 4.2. The former corresponds to a local energy minimum supported by hydrogen bonds which approximates the global energy minimum in the presence of a good solvent, and the latter corresponds to the global energy minimum in the absence of a solvent.

3.2. Force Field. The polymer consistent force field (PCFF)[33] was used in conjunction with recently added parameters for layered silicates.[24,28] PCFF has been designed for organic molecules and yields densities, crystal structures, vaporization energies, and rotational energy barriers[22] mostly in good agreement with experiment. The additional parameters for layered silicates reproduce surface energies and crystal structures in excellent agreement with experiment, as well as approximate vibration frequencies.[29,30]

3.3. Simulation Protocol. In the second half of the NVT molecular dynamics trajectory (section 3.1), snapshots of the trans-configured, duplicate assemblies were recorded. The average basal plane spacing, interlayer density, and the surfactant orientation relative to the surface normal were analyzed. Subsequently, the trans → cis conversion was simulated as described in section 2.2, using temporarily modified force fields over a duration of 200 ps (Figure 4). After the reaction, the assemblies were relaxed using NVT dynamics for 1 ns. In the second half of this trajectory, snapshots of the (predominantly) cis-configured assembly were recorded and the average basal plane spacing, interlayer density, and the surfactant orientation relative to the surface normal were analyzed again. The cis-configured assembly was then subjected to cis → trans conversion as described in section 2.2, followed by NVT dynamics and analysis to examine the reversibility of the reaction.

The basal plane spacing was computed as the difference of the average z coordinate of octahedrally coordinated Al atoms in the two montmorollonite layers (Figure 2), averaged over several hundred snapshots.

The interlayer density was calculated as the quotient of the mass of alkylammonium ions between the silicate layers and the associated interlayer volume. The interlayer volume is calculated according to $V_i = A_i h_i$, where A_i is the cross-sectional area of the box and h_i the interlayer height. The latter is obtained from the basal plane spacing by subtracting the constant value 0.919 nm, equal to the gallery height in pyrophyllite which possesses no charge defects and no interlayer material and is otherwise identical to montmorillonite.[41]

The orientation of the surfactants relative to the surface normal was analyzed qualitatively (visually) and quantitatively. For cation **I**, the distribution of inclination angles of the phenyl rings relative to the {001} montmorillonite surface was computed using 2000 to 6000 independent ring orientations in the series of snapshots of the respective diastereomer. For cations **III** and **IV**, the average tilt angles relative to the {001} surface normal were computed on the basis of the end-to-end vectors (ammonium N atom to 4′-phenyl H atom in cation **III** and ammonium N atom to ammonium N′ atom in cation **IV**, respectively) as an average over at least 4000 independent surfactant orientations in the trajectory. The average refers to absolute individual values, disregarding directional cancelation.

For molecular dynamics simulations in the NVT ensemble, the Verlet integrator, a time step of 1 fs, a temperature of 298 K (maintained through velocity scaling), and a summation of Coulomb and van der Waals interactions using the cell multipole method (fourth order, two layers of cells) were employed, using the Discover program from Accelrys, Inc.[24] For molecular dynamics simulation in the NPT ensemble, the Parrinello-Raman barostat was employed.

4. Simulation Results

In the following, we describe the location and orientation of intercalated flexible (**I** and **II**) and rigid (**III** and **IV**)

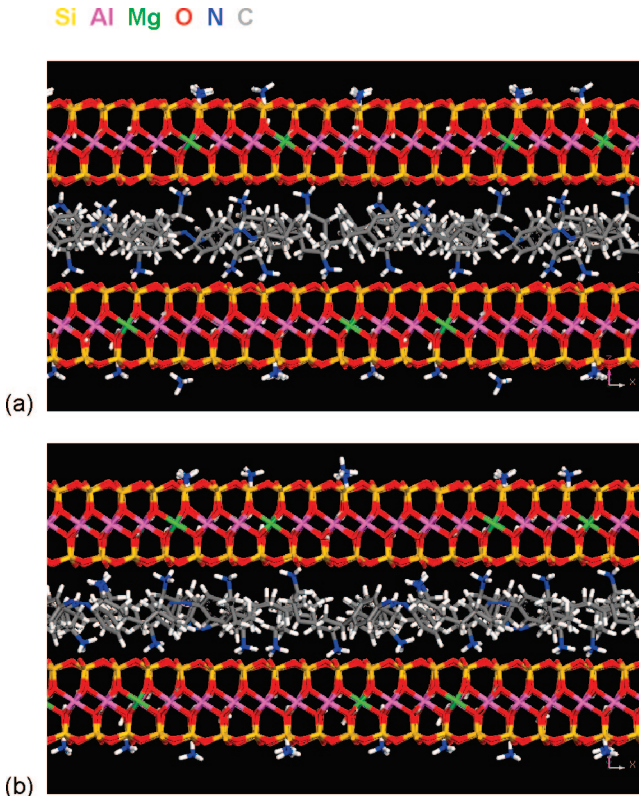

Figure 5. Snapshot of montmorillonite (CEC = 91 mequiv/100 g) modified with a mixture of surfactants **I** (40%) and **II** (60%) perpendicular to the *y* axis. The side view of the (a) trans-configured and of the (b) cis-configured assemblies is very similar.

Table 4. Computed Basal Plane Spacing and Interlayer Density in *n*-Hexylammonium (II) Montmorillonites (CEC = 91 mequiv/100 g) as a Function of the Molar Fraction of C-Terminal Azobenzene (I)

molar fraction of azobenzene (cation **I**)	gallery height in (Å)		interlayer density (kg/m^3)	
	trans	cis	trans	cis
0%	13.95 ± 0.24	13.95 ± 0.24	508 ± 26	508 ± 26
20%	14.68 ± 0.32	14.43 ± 0.16	596 ± 35	624 ± 19
40%	15.29 ± 0.24	15.03 ± 0.21	676 ± 27	706 ± 25
60%	15.50 ± 0.17	15.72 ± 0.18	788 ± 21	762 ± 22

azobenzene derivatives in montmorillonite in the course of the trans−cis isomerization as seen in the simulation.

4.1. Flexible Azobenzene Derivatives. Hybrid structures of montmorillonite (CEC = 91 mequiv/100 g) with *n*-hexylammonium ions (cation **II**) containing 0%, 20%, 40%, and 60% trans-azobenzene at the C-terminal chain ends (cation **I**) have been subjected to trans → cis conversion in molecular dynamics simulation. The reverse cis → trans conversion yields structures equivalent to the original trans-configured assembly.

Representative side views of the trans and of the cis configured structure between the silicate layers are shown in Figure 5 for surfactants with 40% azobenzene content. The computed basal plane spacing for the trans and for the cis configured assemblies shows a transition from a superficial alkyl monolayer with ∼1.4 nm gallery spacing to a partial alkyl bilayer with ∼1.6 nm gallery spacing as the percentage of azobenzene increases (Table 4). Structural changes are similar to an increase in surfactant chain length from C_6 to C_{11} in the absence of azobenzene.[30] In the side

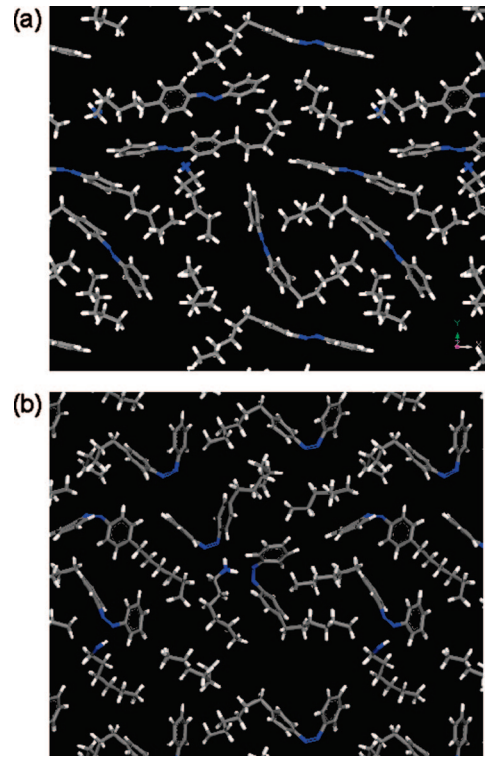

Figure 6. Interlayer structure of montmorillonite (CEC = 91 mequiv/100 g) loaded with surfactants **I** (60%) and **II** (40%), viewed along the *z* direction. The layered silicate structure is omitted in this view. (a) The trans isomer and (b) the cis isomer are conformationally flexible so that a similar basal plane spacing results.

view (Figure 5), no significant differences between the trans and the cis configured surfactants are seen, and the computed basal plane spacing remains the same upon trans−cis conversion within the usual thermal fluctuation,[44,45] represented by the standard deviation (Table 4). The interlayer density increases from ∼510 kg/m^3 for *n*-hexyl ammonium surfactants with no azobenzene content to ∼770 kg/m^3 for a surfactant mixture with 60% azobenzene content, which reflects the higher bulk density of azobenzene and the tendency toward denser packing as the amount of interlayer material per surface area increases, in agreement with previously reported interlayer densities.[30]

The top view onto the interlayer structure for a surfactant mixture, which is shown with 60% azobenzene content (60% mole fraction of surfactant **I**) in Figure 6, explains the structural changes between the trans and the cis configuration. Both isomers are flexible to achieve close packing in the hydrocarbon environment, and the rotation of substituents about the central N=N bond during the trans → cis conversion is supported by simultaneous rearrangements of the flexible alkyl chains in the interlayer space. Virtually no phenyl ring is oriented parallel to the surface (Figure 6), and the significantly tilted orientation relative to the layered silicate surface prevents an expansion of the gallery perpendicular to the layered silicate plane upon photoisomerization. The statistical analysis reveals more details of the orientation of the phenyl rings relative to the {001} surface plane upon

(44) Osman, M. A.; Ploetze, M.; Skrabal, P. *J. Phys. Chem. B* **2004**, *108*, 25280–25288.
(45) Jacobs, J. D.; Koerner, H.; Heinz, H.; Farmer, B. L.; Mirau, P. A.; Garrett, P. H.; Vaia, R. A *J. Phys. Chem. B* **2006**, *110*, 20143–20157.

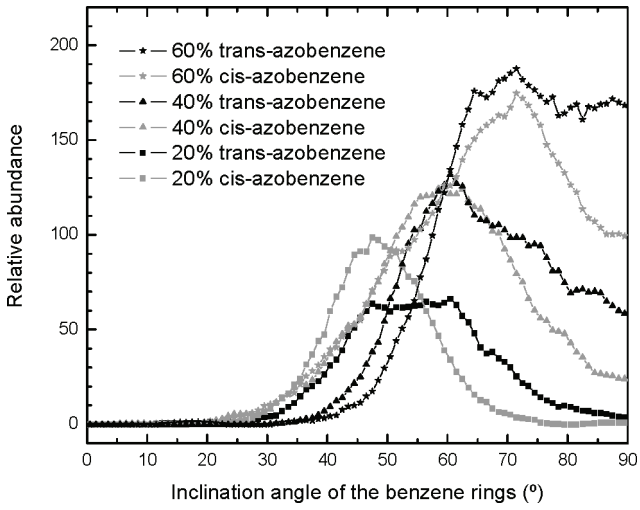

Figure 7. Distribution of the inclination angles of the phenyl rings relative to the {001} surface plane in mixtures of cations **I** and **II** bound to montmorillonite (CEC = 91 mequiv/100 g). Average inclination angles range from 55° to 70° in trans-azobenzene and are slightly lower in cis-azobenzene. Parallel orientation of the phenyl rings to the surface appears unfavorable.

trans → cis conversion (Figure 7). The average inclination of the phenyl rings relative to the {001} surface plane increases from 55° to 70° as the mole fraction of trans-azobenzene increases from 20% to 60% in the mixture of cations **I** and **II.** The phenyl rings in cis-azobenzene exhibit on average ~6° less inclination relative to the mineral {001} surface than in trans-azobenzene, and high inclination angles between 70° and 90° are less frequently seen.

In summary, the interlayer environment supports the quantitative isomerization of azobenzene (Figure 6b) and conformationally flexible azobenzene-containing surfactants at low packing density exhibit only minor changes in gallery spacing upon photoisomerization on the order of few percent which are within the typical range of variations in interlayer density due to thermal fluctuation and annealing.[30,44,45]

4.2. Rigid Azobenzene Derivatives. Hybrid structures of montmorillonite (cation exchange capacity CEC = 143 mmol/100 g) and the azobenzene derivatives **III** and **IV** have been subjected to trans → cis conversion in molecular dynamics simulation using two distinct setups, one with upright orientation of the dye molecules on the surface in vacuum (equal to the presence of an implicit solvent), and another with a dense interlayer structure (equal to the absence of a solvent). The reverse cis → trans conversion yields structures equivalent to the original trans-configured assembly in all instances.

In the setup with upright orientation of the cations **III** and **IV** on the surface, the presence of a good solvent is necessary to fill the remaining interlayer space for thermodynamic stability. While no explicit solvent was included in the simulation, vacuum assumed the role of a good implicit solvent due to the high energy barrier relative to the structure of high interlayer density (section 3.1). We consider the good solvent miscible with azobenzene and with montmorillonite to fill the remaining vacuum, while a poor, immiscible solvent would lead to a dense interlayer just as if no solvent is present. Thus, under good solvent conditions, representative snapshots of the azobenzene-modified layered silicates in the trans and in the cis configuration (Figure 8) show the stiff molecular axis of surfactants **III** and **IV**, as well as three hydrogen bonds between primary ammonium head groups and oxygen atoms in the cavities of the clay mineral surface.[28,30] This configuration leads to substantial reversible changes in gallery spacing upon trans → cis isomerization (Table 5). The medium-to-high cation density of the mineral (143 mequiv/100 g) causes a substantial packing density of the surfactants and supports the alignment of the rigid backbones close to the surface normal. Differences in gallery spacing upon isomerization amount to 2.2 Å or 11% for (4-phenylazophenyl)ammonium ions (**III**) and to 2.8 Å or 14% for (4,4′-phenylazophenyl)diammonium ions (**IV**). The extent of switching is thus similar to the change in length of an azobenzene molecule during isomerization (2.3 Å), and the presence of ammonium groups at both ends of the azobenzene in cation **IV** increases the switchable length compared to azobenzene with one freely movable end in cation **III**. The analysis of the average tilt angle of the cations **III** and **IV** relative to the surface normal (Table 5) shows some deviation from ideal upright orientation (0°), in spite of the preference of the primary ammonium head groups for tripod arrangements on the silicate surface (Figure 8).[30] In the trans configuration, the monocations **III** exhibit a higher tilt angle (24°) than that of the dications **IV** (9°) due to an unbound C-terminal end. Upon isomerization, the molecules twist which results in higher end-to-end tilt angles of 58° and 24°, respectively. When we consider the directional average of the tilt angles over all surfactants on the surface, a value near 0° is found for all trans and cis configured systems due to random orientation of individual surfactant backbones.

The setup with a dense interlayer structure is thermodynamically stable in the absence of solvents. In montmorillonite-**III**, the trans and the cis isomers display gallery spacings of 20.0 Å and 17.6 Å, which are practically the same as in the upright orientation (Table 5) and correspond to interlayer densities of 694 ± 13 kg/m^3 and 892 ± 21 kg/m^3. Therefore, the medium-to-high packing density and the conformational rigidity of the trans-configured backbone support reversible actuation and associated changes in interlayer density also in the absence of a solvent. Particularly, the cis configuration leads to dense interlayer packing (Figure 8b). Under a pressure of 1 GPa, the basal plane spacing of the trans isomer could be compressed to 16.6 Å (interlayer density 1010 kg/m^3) in NPT molecular dynamics; however, it returned to a gallery spacing of 20.0 Å under pressures ≤ 1 MPa. Within the accuracy of the force field, the simulation thus confirms significant actuation for montmorillonite-**III**. The trans and the cis isomer of montmorillonite-**IV** with densely packed interlayer structure display a variable gallery spacing of 14−15 Å (trans) and 13.2 Å (cis), which demonstrates significant compression compared to the upright orientation of the dye molecules (Table 5). The compression is associated with a 50% lower packing density of the dication **IV** on the surface compared to the monocation **III** (see Figure 8c vs Figure 8a). In this densely packed configuration, the interlayer densities amount to 840−670 kg/m^3 (trans) and 1010 ± 50 kg/m^3 (cis), and the bidentate cation **IV** shows two distinct binding modes to the surface

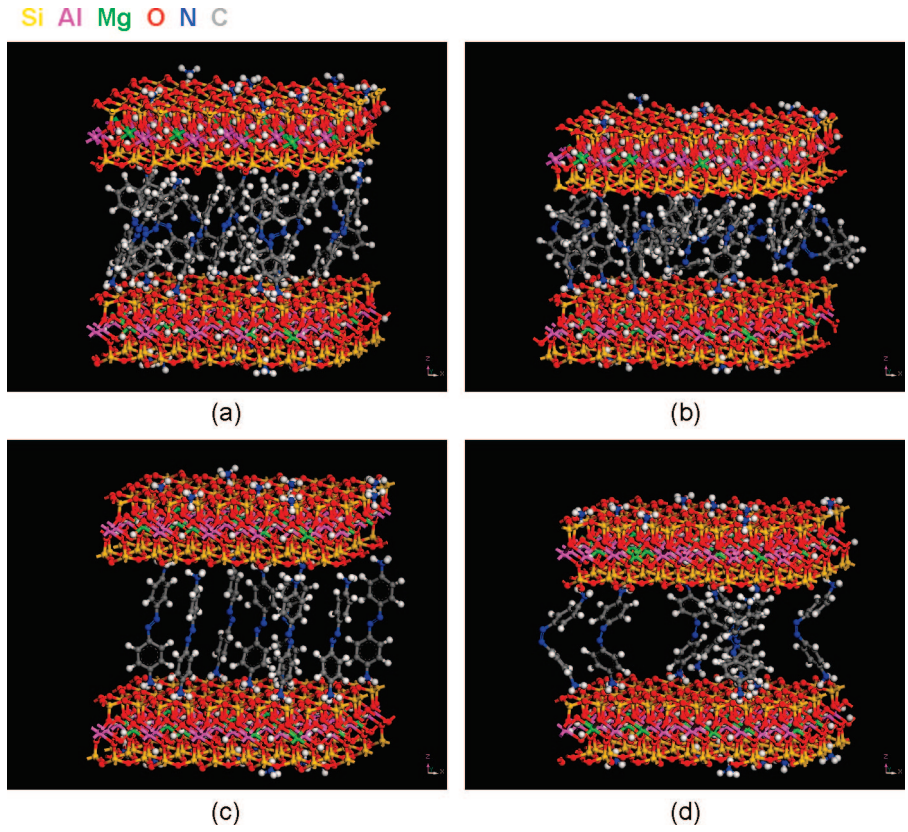

Figure 8. Snapshots of montmorillonite (CEC = 143 mequiv/100 g) modified with surfactants **III** and **IV** in near-upright orientation on the surface, showing significant actuation upon photoisomerization. (a) Trans-azobenzene and (b) cis-azobenzene in montmorillonite-**III**. (c) Trans-azobenzene and (d) cis-azobenzene in montmorillonite-**IV**.

Table 5. Computed Gallery Spacing and Average End-to-End Tilt Angles Relative to the Surface Normal for Montmorillonite (CEC 143 mequiv/100 g) Modified with Azobenzene Derivatives III and IV in Near-Upright Orientation on the Surface

	cation **III**		cation **IV**	
	gallery height (Å)	tilt angle (deg)	gallery height (Å)	tilt angle (deg)
trans	19.98 ± 0.16	27 ± 2	20.62 ± 0.13	9 ± 2
cis	17.81 ± 0.19	58 ± 3	17.79 ± 0.27	24 ± 2
difference	±2.17 (11%)	31	±2.83 (14%)	15

(Figure 9): bridging (cross-links) between two silicate layers through an ionic bond to each layer, similar as in Figure 8 c,d, or flat on one silicate layer through two ionic bonds to the same layer. The ratio of the binding modes does not seem to affect the gallery spacing of cis-configured montmorillonite-**IV** (13.2 Å); however, the gallery spacing of trans-configured montmorillonite-**IV** is affected. For example, 25% cross-linking leads to 14.0 Å and 50% cross-linking to 15.0 Å gallery spacing. Under a pressure of 1 GPa, the trans-configured interlayer could be compressed to a gallery spacing of ~12.8 Å (interlayer density 1120 kg/m^3) and returned to the original gallery height upon relief of the pressure. Overall, montmorillonite-**III** and montmorillonite-**IV** in the cis configuration possess a lower basal plane spacing, a higher interlayer density, and a higher tilt angle of the azobenzene backbones relative to the surface normal. This is related to the twisted, sterically less demanding geometry of the cis isomers. On the contrary, the rigid trans isomers are sterically more demanding and induce a higher gallery spacing.

In summary, conformationally rigid azobenzene derivatives have the potential to achieve significant reversible changes in gallery spacing, supported by vertical alignment on the surface. The compensation of fluctuations in interlayer density upon photoisomerization through the presence of a good solvent with the ability to exit from or enter into the gallery, as in the case of upright orientation on the surface, can play a significant role to control and increase reversible changes in gallery spacing.

5. Comparison with Experiment

In the following, we compare the simulation results for the intercalated cations **I** to **IV** to available experimental data. Flexible (**V**) and semiflexible surfactants (**VI** and **VII**) have been employed in experiment (Scheme 2)[17−20] while rigid surfactants have not yet been investigated to our knowledge. Various layered silicates have served as surfaces, including montmorillonites $K_x[Si_2O_4][Al_{2-x}Mg_xO_2(OH)_2][Si_2O_4]$,[15,16,19,20] saponite $(1/2\ Ca, Na)_x[Si_{2-x/2}Al_{x/2}O_4][(Mg, Fe^{II})_3O_2(OH)_2][Si_{2-x/2}Al_{x/2}O_4]$,[15,16,20] and synthetic minerals such as fluor-tetrasilicic mica $Na_x[Si_2O_4][Mg_{3-x}Na_xO_2F_2][Si_2O_4]$ (TSM)[20] and Li fluor-taeniolite $Li_x[Si_2O_4][Mg_{3-x}Li_xO_2(OH)_2][Si_2O_4]$.[18] For the same x, these minerals possess almost the same surface geometry, the same number of single charged cations per surface area A_S^{-1}, approximately the same CEC, and almost the same structure and dynamics of given attached ammonium surfactants.[31] For example, $x = 1$ leads to a cation density $A_S^{-1} = 2.14$ nm^{-2} and CEC = 251 mmol/100 g (muscovite mica) and $x = 0.5$ leads to $A_S^{-1} = 1.07$

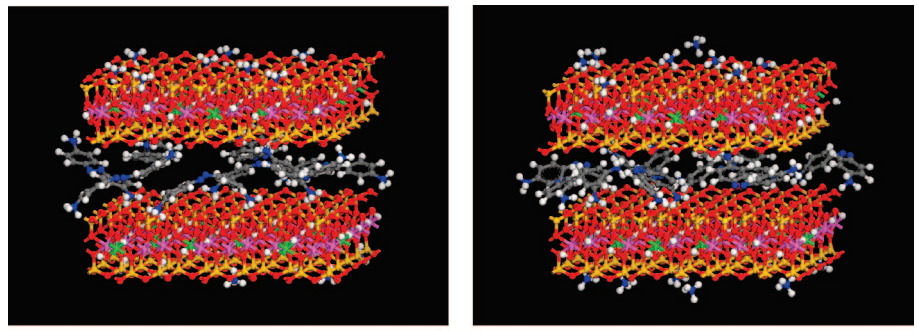

Figure 9. Snapshots of montmorillonite (CEC = 143 mequiv/100 g) modified with surfactant **IV** in dense interlayer packing. (a) Trans configuration and (b) cis configuration. Only a fraction of the cations forms cross-links between the two silicate layers,and the remaining cations are attached to the same silicate layer with two ionic bonds, which reduces changes in gallery spacing upon photoisomerization.

Scheme 2. Cationic Surfactants Employed in Experiment (refs 17−20)

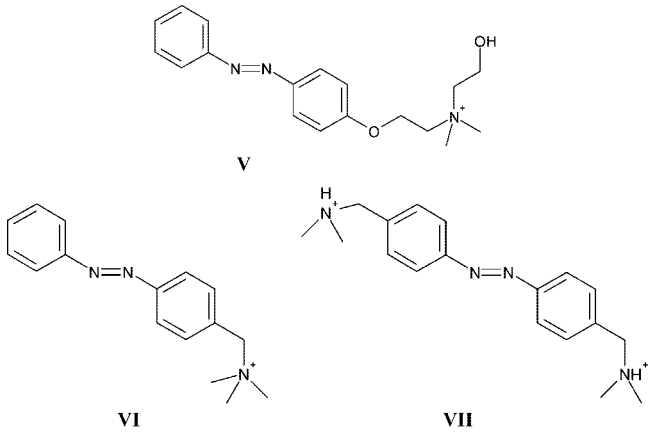

nm^{-2} and CEC = 134 mmol/100 g (montmorillonite).[31] Magadiite $Na_1[Si_7O_{14}(OH)]\cdot nH_2O$ has also been employed and resembles mica-type silicates in cation density A_S^{-1} = 1.90 nm^{-2} and in CEC ∼220 mequiv/100 g,[17] although the surface geometry is different.[15−17]

The number of cations per surface area A_S^{-1} is more appropriate to describe the formation of self-assembled structures[31] than the molar quantity of exchangeable cations per unit mass of mineral (CEC). Nevertheless, we employ the CEC (in mmol single charged ions per 100 g) to compare the mineral surfaces since the CEC is yet more common in the experimental literature and proportional to the cation density A_S^{-1} within ±10% (the exact conversion from CEC into A_S^{-1} requires knowledge of the crystal structure and the stoichiometry of the minerals). Since the composition of the minerals and the CEC are associated with uncertainties up to ±10%,[17−20,22,31] the following discussion of experimental data is of semiquantitative nature.

5.1. Flexible Azobenzene Derivatives. Layered silicates modified with 2-hydroxyethyl-2-(4-oxophenylazophenyl)ethyldimethylammonium ions (**V**) have been extensively investigated.[17,19,20] At low CEC and azobenzene loading levels similar to those in section 4.1, the absence of reversible changes in gallery spacing upon laser excitation was found[19,20] while UV/vis absorption spectra indicated near-quantitative conversion by photobleaching of respective absorptions at ∼345 nm (trans) and ∼420 nm (cis), irrespective of loading level. Reactions were typically completed within 10 min of irradiation. Simulation results (Table 4) for the similar cations **I** and **II** agree with the observations and offer further insight as follows.

(1) Ogawa et al.[19] investigated cation **V** on montmorillonite of a cation exchange capacity (CEC) 119 mequiv/100 g. Nonquantitative cation exchange corresponding to 13, 37, 66, 94, and 105 mequiv/100 g resulted in a basal plane spacing of 13.3, 15.0, 15.3, 16.9, and 18.6 Å. None of these systems showed significant changes in gallery spacing after UV irradiation at the photostationary states while nearly quantitative reversible photoisomerization was demonstrated by changes in the UV/vis spectra. The amount of azobenzene loading increased from 11%, 31%, 55%, 80%, to 88% in these systems, and the measured gallery spacing agrees with the computed values in Table 4 for corresponding azobenzene loading, taking into account some differences in the structure of the cations (**I/II** vs **V**) and in CEC. Okada et al.[20] further examined cation **V** on saponite and montmorillonite with total cation exchange capacities of 71 and 105 mequiv/100 g. Subquantitative and superquantitative cation exchange corresponding to 66 mequiv/100 g (montmorillonite), 76 mequiv/100 g (saponite), and 91 mequiv/100 g (montmorillonite) resulted in a constant basal plane spacing of 15.4 Å, 15.7 Å, and 15.4 Å for the trans isomer and for the cis isomer after UV irradiation. The computed basal plane spacing for montmorillonite of CEC 91 mequiv/100 g with surfactants **I** and **II** containing 40% to 60% azobenzene (Table 4) yields similar values of 15.3 to 15.5 Å so that changes in molecular structure upon isomerization can be compared to Figures 5 and 6 in first approximation. The gallery spacing corresponds to an intermediate state between flat alkyl monolayers and flat alkyl bilayers on the surface.[30] In the experimental system of 91 mequiv/100 g, addition of an excess amount of phenol (four times the mass of montmorillonite-**V**) caused a second XRD peak at 25.6 Å before (trans) and after UV irradiation (cis), and a third, irreversible peak emerged at 34 Å after UV irradiation (cis).[20] Cointercalates therefore show the potential to increase significantly reversible changes in gallery height upon trans−cis conversion. However, the 8.4 Å gallery expansion upon isomerization with cointercalated phenol was only observed in partial yield and in select systems.[20]

(2) The interaction of the azobenzene derivatives with the montmorillonite surface causes a bathochromic shift of the

UV absorption relative to the reference state in solution (342 nm). This spectral shift ranges between +0 and +10 nm and increases with the amount of surface contact between azobenzene and the tetrahedral silicate sheet, for example, in the order of decreasing amount of ion exchange and decreasing packing density.[19,20,31,46,47] Upon isomerization, however, the distinct UV absorption of trans-azobenzene disappears and the change in orientation relative to the surface cannot be followed in this manner. Molecular dynamics results suggest the orientation of phenyl rings relative to the surface to be preferably between 45° and 90° for trans-azobenzene, with a trend toward 90° at high loading, and a slight decrease by ~6° upon conversion to the cis isomer (section 4.1, Figure 7).

(3) Experimental data have also been obtained for the flexible surfactant **V** at higher packing density on layered silicate surfaces of CEC 94, 108, and 220 mequiv/100 g.[17,20,31] The flexible surfactant **V** was grafted to surfaces of montmorillonite of CEC = 108 mequiv/100 g and to a tetrasilicic mica of CEC = 94 mequiv/100 g.[20] The higher packing density leads to organic bilayer structures[30] with basal plane spacings of 17.6 Å and 18.9 Å for the trans isomers, respectively. The surfactant backbone is then only in contact with one of the two silicate surfaces (unlike Figure 5), supported by a smaller UV redshift from 342 nm in solution to 345 and 344 nm in the trans-hybrid structures (unlike 349 nm at a CEC of 71 mequiv/100 g).[20] Bleaching of the characteristic UV adsorption confirmed isomerization; however, no reversible changes in gallery spacing were found upon UV stimulation unless a fourfold mass excess of phenol was added. In the presence of phenol, reversible but nonuniform changes in gallery spacing occurred from 25.6 Å and 24.5 Å of the cointercalated assembly (trans) to 31.6 Å and 34.5 Å (cis), respectively. Similar as reported under (1), the gain in gallery height for the cis isomer originates from the preferential solvation of cis-azobenzene by phenol through hydrogen bonds and an influx of the cointercalate into the gallery.[20] Further, magadiite, CEC of 220 mequiv/100 g, and cation **V** yield structures with reversibly switchable basal plane spacing from 26.9 Å (trans) to 27.5 Å (cis).[17] Given the high basal plane spacing, the backbones of cation **V** possess a small tilt angle relative to the surface normal[25] and experience π-stacking interactions. These are evidenced by a blueshift (instead of a redshift) of the absorption from 342 nm in solution to 335 nm on magadiite.[46] This example illustrates that very dense packing and quasi-crystalline orientation of the dye molecules limit the potential of actuation. It may be possible, however, to increase minor reversible changes (~2%) by addition of a suitable cointercalate.

5.2. Semi-Flexible Azobenzene Derivatives. Layered silicates of medium-to-high cation exchange capacity, quantitative loading, and semiflexible surfactant structure[17,18,20] show quantitative photoisomerization and basal plane distances similar as discussed in section 4.2 for densely packed rigid surfactants. The changes in gallery spacing upon isomerization, however, are smaller for the semiflexible surfactants, and no significant reversible actuation is found.

A synthetic montmorillonite of a CEC = 157 mequiv/100 g with trimethyl-(4-phenylazophenyl)methylammonium ions (**VI**) yields 22.2 Å basal plane spacing in the trans-configuration, and the gallery spacing was irreversibly switchable from 22.2 Å (trans) to 21.3 Å (cis).[18] The experimental gallery height is similar to computed values of 20.0 Å (trans) and 17.6 Å (cis) for cation **III** in section 4.2, taking into account a higher CEC and a slightly longer chain in experiment. However, clearly a smaller difference of 0.9 Å in gallery spacing is experimentally found related to the residual flexibility of the backbone in cation **VI** (an alkyl spacer is present and no hydrogen bonding of the headgroup to the surface is possible)[30] compared to 2.4 Å in the simulation of the conformationally rigid cation **III**. Although the presence of a solvent was not required in the simulation, a solvent would likely support the compensation of changes in interlayer density for increased actuation (Table 5 and Figure 8 a,b). The lack of reversibility of the switching in gallery height in experiment could be associated with improved packing of the cis isomers which then convert back to the trans configuration without a significant change in location and without noticeable expansion.

The same synthetic montmorillonite of a CEC = 157 mequiv/100 g with 4,4′-phenylazophenyl-bis(*N*,*N*′-dimethylmethyleneammonium) ions (**VII**) yields 15.02 Å basal plane spacing in the trans form, and the gallery spacing was reversibly switchable from 15.02 Å (trans) to 14.92 Å (cis). The bidentate cation **VII** assumes only half the packing density compared to the monodentate cation **VI** (see Figure 8c vs Figure 8a for the analogy of cations **IV** and **III**). The measured low gallery height is in agreement with the computed values of 14−15 Å (trans) and 13.2 Å (cis) for montmorillonite-**IV** with dense interlayer structure (Figure 9), under consideration of the longer chain and the higher CEC in experiment. The small change of 0.1 Å in gallery height in experiment is consistent with the residual flexibility of cation **VII** (two alkyl spacers and diminished hydrogen bonding ability of the head groups)[30] compared to the stiff cation **IV**. The presence of a cointercalate could also support an upright orientation with up to 2.8 Å actuation (Table 5, Figure 8 c,d).

In summary, small changes in gallery height of semiflexible surfactants may be increased to between 2 Å and 2.5 Å, or ~10% of total gallery spacing, if a suitable cointercalate is present and if the surfactants become of rigid geometry with a thermodynamic bias toward upright orientation, as suggested by replacement of cation **VI** with cation **III** and of cation **VII** with cation **IV**.

5.3. Relation between Structure and Reversible Switching. Experiment and simulation show that flexible azobenzene-containing surfactants at low packing density do not yield reversible changes in gallery spacing due to the ease of chain rotation and available lateral space in the gallery. The minimum free energy of dye-modified layered silicates is then associated with an optimum interlayer density determined by packing constraints. Significant changes in the interlayer density associated with vertical movement of

(46) Heinz, H.; Suter, U. W.; Leontidis, E. *J. Am. Chem. Soc.* **2001**, *123*, 11229–11236.
(47) Leontidis, E.; Heinz, H.; Palewska, K.; Wallenborn, E.-U.; Suter, U. W. *J. Chem. Phys.* **2001**, *114*, 3224–3235.

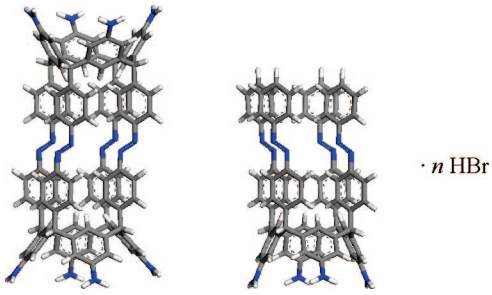

Figure 10. Potential azobenzene derivatives to support reversible changes in gallery spacing when grafted to layered silicate surfaces.

silicate layers (>5%) must be offset by cointercalate such as a fluid which can enter into the gallery upon expansion and retreat from the gallery upon contraction. Rigid trans-azobenzene derivatives are sterically demanding and support decreased interlayer densities, while the corresponding rigid cis-azobenzene derivatives are sterically less demanding and favor higher interlayer densities. Experimental evidence shows that cointercalates such as phenol may also switch the gallery height significantly in excess of the "intrinsic" change in geometry of the azobenzene derivatives.[20] For phenol, this is related to preferential solvation of the azobenzene N═N bond in the cis configuration. However, yet only nonuniform, partial amplification of the "intrinsic" difference of the gallery spacing has been observed using solvents.

Without the expectation of amplified switching due to cointercalates, the simulation shows that an upright orientation of the surfactants on the layered silicate surfaces with medium-to-high packing density can raise intrinsic actuation above 10% of the gallery spacing (Figure 8), especially when combined with a good solvent or cointercalate. Yet few azobenzene-based surfactants with a thermodynamic preference for the desired vertical orientation on the surface and equally few synergistic cointercalates have been tested. Tailor-made surfactants could provide control over interlayer structure and actuation; for example, the compounds shown in Figure 10 could benefit from multiple ion exchange for rigid grafting to the layered silicate surface. In the simpler cations **III** and **IV**, phenyl groups next to the azo group can also be replaced by biphenyl or fused ring systems to increase the switchable length.[14]

Experimental and simulation data further indicate that very high packing densities on the surface (leading to nearly vertically oriented layers) might limit actuation due to steric hindrance. However, the isomerization reaction itself appears to be unaffected by the confinement of the azo dyes unless very high pressures (>1 GPa) are applied (section 2).

6. Summary

From a methods viewpoint, a classical molecular dynamics approach to simulate the trans−cis isomerization of azobenzene and its derivatives has been described. The procedure is based on a temporary modification of the torsion potential to model the impact of photon energy and is compatible with common force fields containing three-term torsion potentials and one-term torsion potentials. By feeding UV spectroscopic data and ab initio understanding of the isomerization reaction into the model, it accounts for the input of excitation energy, the time scale of the reaction, and the relative energies of the trans and of the cis isomer, as well as for the barrier of thermal conversion. As indicated for simple azobenzene test systems, it is possible to retrieve details about the reaction dynamics and to probe the sensitivity to external pressure, temperature, and approximate excitation time (duration and number of laser pulses), as well as the molecular environment in large systems.

The simulation approach has been applied to explain changes in the basal plane spacing of layered silicates with ammonium-functionalized, azobenzene-containing surfactants upon photoisomerization by simulation and comparison to XRD and UV/vis spectral data. The trans−cis isomerization takes place quantitatively in the constrained geometries, and the isomerization reaction has been examined for flexible, semiflexible, and rigid azobenzene derivatives. Conformational flexibility of intercalated azo dyes facilitates molecular rotation and causes small to no changes in gallery spacing upon photoisomerization unless differences in solvation energy between the two isomers are exploited through addition of a cointercalate. In contrast, conformational rigidity of the intercalated azo dyes supports reversible actuation in the interlayer space upon isomerization, particularly in near-upright orientation on the surface. Rigid trans isomers are found to be sterically more demanding than the corresponding cis isomers which arrange flexibly into dense interlayer structures. The use of rigid dications to achieve changes in gallery spacing upon photoisomerization is more effective when they act as cross-links between two silicate layers and less effective when they are doubly bonded to one layer. Significant controllable actuation also depends on, or is supported by, the presence of cointercalates which can reversibly enter into and exit from the interlayer space.

In conclusion, simulation results indicate that experimentally achieved reversible changes in gallery spacing of 0.9 Å (4%) may be improved up to 2.8 Å (14%) through (1) presence of a cointercalate to compensate, and possibly overcompensate, associated changes in interlayer density, (2) conformational rigidity of the azobenzene-containing moieties, and (3) upright orientation of the dye molecules on the surface. A moderate-to-high cation exchange capacity (CEC), the absence of flexible alkyl spacers in the surfactants, and the use of rigid macrocyclic "pedestals" support this objective. Yet few rigid azobenzene derivatives and cointercalates have been explored in the interlayer space, and it is hoped the present work will stimulate further research in this direction.

Acknowledgment. We are grateful to the Air Force Research Laboratory (AFRL), the University of Akron, and Wright State University, Ohio, for support. Discussions with L.R. Drummy (AFRL), T. Kyu, and S.C. Jana (University of Akron) are acknowledged.

CM801287D